Design of High-Temperature, Gas-Phase Synthesis of Hard or Soft TiO_2 Agglomerates

Robert N. Grass, Stavros Tsantilis, and Sotiris E. Pratsinis
Particle Technology Laboratory, Institute of Process Engineering, Dept. of Mechanical and Process Engineering (D-MAVT), ETH Zürich, Sonneggstrasse 3, ML F25 CH-8092 Zurich, Switzerland

DOI 10.1002/aic.10739
Published online December 29, 2005 in Wiley InterScience (www.interscience.wiley.com).

Conditions for high temperature, aerosol synthesis of titania (TiO_2) with controlled degree of agglomeration are identified. Accounting for simultaneous gas phase and surface reactions, coagulation and sintering during formation and growth of titania by oxidation of Ti-tetraisopropoxide (TTIP) and $TiCl_4$ vapors, the evolution of the primary particle and agglomerate collision diameters is presented at nonisothermal conditions neglecting the polydispersity of the particle-size distribution. Hard- or soft-agglomerate formation is identified at the end of full coalescence and sintering, respectively. The role of surface reaction on the evolution of the agglomerate state is examined. Diagrams for the degree of hard-agglomeration as well as the size of the primary TiO_2 particles are developed in terms of maximum process temperature, cooling rate and precursor initial molar fraction and compared with experimental data on synthesis of nonagglomerated TiO_2. © 2005 American Institute of Chemical Engineers *AIChE J,* 52: 1318-1325, 2006
Keywords: aerosol, degree of agglomeration, sintering, nanoparticles, structure

Introduction

Titania particles are used mostly as white pigments and opacifiers in paints and to a lesser extent as catalysts and polymer fillers. About half of the world's production of TiO_2 takes place by gas phase oxidation of $TiCl_4$ in flame aerosol reactors by the so-called "chloride" process. There, typically, agglomerates are formed that are broken later on by grinding into the constituent primary particles. For pigments and most of other applications, close control of titania particle size, crystallinity and degree of agglomeration is needed.

Control of crystallinity is reasonably well understood as certain additives promote the rutile or anatase phase through substitutional or interstitial crystal lattice defects.[1] Recently, there have been significant advances in understanding titania formation in flames so that the evolution of primary particle size can be predicted from first principles without any adjustable parameters given the particle temperature history, especially in uniform premixed flames.[2] In addition, product agglomerate size distributions are reasonably well understood as these fractal-like structures attain self-preserving distributions by Brownian coagulation.[3]

In contrast, controlling the agglomerate structure has been rather challenging. This is important for pigments and composites where nonagglomerated particles are needed, while in catalysis, agglomerated ones are desired to assure loose packaging and small pressure drop through the final catalyst pellet. Frequently, post processing such as grinding is used to reduce agglomerate size increasing cost and introducing impurities. The difficulty in understanding agglomerate dynamics can be traced to the lack of consistent data. Agglomerate size and structure are rather sensitive during sampling for *ex situ* measurements (microscope counting or electrical mobility analysis) or data inversion for *in situ* measurements making difficult an undisputable agglomerate size and structure estimation. This sensitivity can be traced to the robustness of agglomerate structure. Agglomerates made of primary particles bound with hard (sintering) bonds tend to withstand sample preparation

Correspondence concerning this article should be addressed to S. E. Pratsinis at sotiris.pratsinis@ptl.mavt.ethz.ch.
Current address of R. N. Grass: Institute for Chemical and Bioengineering, ETH Zurich, 8093 Zurich, Switzerland.
Current address of S. Tsantilis: Cilag AG (Johnson & Johnson), Hochstrasse 201, 8205 Schaffhausen, Switzerland.

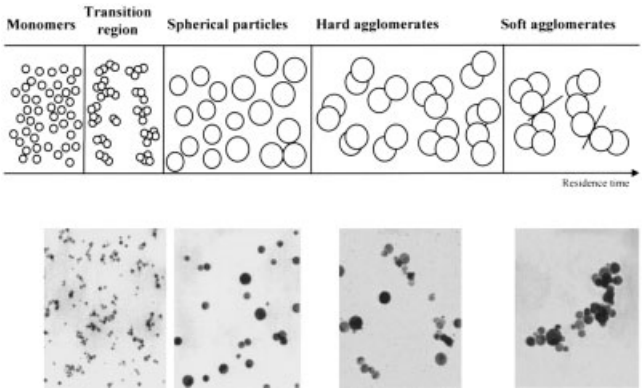

Figure 1. Agglomerate particle formation sequence in aerosol processes adapted from Kruis et al.[7] along with characteristic TEM images from Arabi-Katbi et al.[5]

while softly-bound ones with physical (for example, van der Waals) forces tend to be easily disrupted.

From a manufacturing point of view, hard-agglomerates require far more energy for breakup than soft-ones. In addition the former can be detrimental in polishing applications introducing surface defects (scratches). Although the distinction between hard- and soft-agglomerates is largely empirical, very recently it was proposed that the effective end of sintering during particle formation can be used to signify the onset of soft-agglomerate formation upon collision. Using this distinction, process parameters leading to the formation of soft-, hard- and even nonagglomerate silica particles made by $SiCl_4$ oxidation could be identified accounting for aerosol coagulation and sintering.[4]

Here, the latter study is extended to gas-phase synthesis of titania exploring, in particular, the significance of surface growth (precursor oxidation on particle surface) on the evolving agglomerate structure. Furthermore, maps of the degree of hard-agglomeration are developed in terms of maximum process temperature, flame cooling rate and precursor inlet concentration and compared to data of synthesis of hard- or nonagglomerated titania nanoparticles. Finally, process conditions for synthesis of hard-agglomerated titania are compared to those of silica pointing out the significance of material properties in selection of such conditions.

Theory

Titania precursor gas ($TiCl_4$ or TTIP) is oxidized forming clusters of tiny primary particles that fuse and may fully coalesce forming single particles upon passing through the highest flame temperature.[5] Later on, these particles re-agglomerate as the flame cools downstream and the rate of particle coalescence (sintering) becomes slower than that of particle collision resulting in fractal-like agglomerates (Figure 1). When coalescence (sintering) is faster than collision, nonagglomerate, single particles are formed.[6] When the reverse takes place, agglomerates are formed that are either hard when sintering is slower than particle collisions, or soft when sintering has ceased completely.[4]

Aerosol dynamics

This process is described quantitatively by precursor oxidation (in the gas phase or on the newly formed particle surface, such as surface growth), coagulation and sintering assuming monodisperse primary and agglomerate size distributions.[2,7] The monodispersity gives little error (up to 15%) with respect to average particle properties (namely, primary particle and agglomerate collision diameters and number of primaries per agglomerate) when chemical reaction is complete[8] and a unimodal distribution has been formed,[2] when compared to more accurate sectional[9] or bimodal[10] models. As a result, it has been used successfully in detailed aerosol reactor modeling by combining computational fluid mechanics and titania particle dynamics (hot-wall reactors: Schild et al.[11]; flame reactors: Johannessen et al.[12]).

Thus, the evolution of precursor, C (molecules/g-gas), particle number, N (particles/g-gas), agglomerate surface area, A (cm^2/g-gas), and volume, V (cm^3/g-gas), concentrations are[2]

$$\frac{dC}{dt} = -kC = -(k_g + k_s A \rho_g)C \tag{1}$$

$$\frac{dN}{dt} = -\frac{1}{2}\beta N^2 \rho_g + k_g C \tag{2}$$

$$\frac{dA}{dt} = k_g C \alpha_m - \frac{1}{\tau_{\sin}}(A - N\alpha_s) + 4\pi N n_p d_p (k_s C \rho_g) v_m \tag{3}$$

$$\frac{dV}{dt} = kCv_m \tag{4}$$

where v_m (cm^3) and α_m (cm^2) are, respectively, the sphere-equivalent volume and surface of a titania molecule, ρ_g (g/cm^3) is the density of the carrier gas and α_s (cm^2) is the surface area of the agglomerate volume-equivalent sphere. The characteristic sintering time for titania, $\tau_{\sin}$ (s) is[13]

$$\tau_{\sin} = 7.4 \cdot 10^8 d_p^4 T \exp\left(\frac{31000}{T}\right) \tag{5}$$

while the Brownian coagulation rate, β (cm^3/s), is given by the Fuchs interpolation from the free-molecular to the continuum regime.[4,7,14] The total, gas phase and surface reaction rate constants k (s^{-1}), k_g (s^{-1}) and k_s (cm/s), respectively, for a precursor are given later.

The agglomerate properties are calculated assuming that all agglomerates are equal and consist of spherical primary particles of equal dia. d_p (cm), while the agglomerate collision dia. d_c (cm), is related to the number of primary particles n_p, and the mass fractal dimension D_f.[4,7] The collision diameter at the end of sintering (the time t at which the primary particle dia. d_p, is within 1% of its final value d_{pF}, so, $d_p = 0.99\ d_{pF}$) is defined as the hard-agglomerate collision dia. d_H. Finally the degree of hard agglomeration is $h = d_H/d_p$ at the end of the sintering period of the process, for example, when d_p no longer effectively changes.[4] For $h = 1$ there are no agglomerates. Increasing h reflects an increased extent of agglomeration.[4] The characteristic time for coagulation, τ_c (s) is[6]

$$\tau_a = \frac{2}{\beta \rho_g N} \tag{6}$$

Reaction kinetics

The thermal decomposition of TTIP to TiO_2 ($TTIP_{gas} \xrightarrow{k} TiO_2 + 4C_3H_6 + 2H_2O$) has a rate constant of[15]

$$k = 3.96 \times 10^5 \exp\left(\frac{-8480}{T}\right) \tag{7}$$

where T(K) is the gas temperature. The surface growth rate of TTIP is based on a first-order surface reaction[2,16] with

$$k_s = 1 \times 10^{11} \exp\left(-\frac{15155}{T}\right) \tag{8}$$

Furthermore, the rate of the gas phase reaction is[2]

$$k_g = k - k_s A \rho_g \tag{9}$$

It should be noted that these reaction rate constants have been measured at temperatures lower than typically encountered in flame reactors. In addition, water can be produced during combustion, thus promoting TTIP hydrolysis. Nevertheless in all cases considered here complete conversion of the TiO_2 precursor has been achieved.

Agglomerate structure

The agglomerate structure is described quantitatively by the so-called mass fractal dimension D_f, as it is commonly done in agglomerate aerosol dynamics[17] although this may have some limitations.[18] As shown previously[7], β depends on d_c and, hence, on D_f. For agglomerates made by cluster-cluster collisions $D_f = 1.8$ or 2.4 for monomer-cluster collisions.[17] In most models D_f is constant although experiments[19] and Monte Carlo simulations[20] show that it takes some finite time till D_f reaches that constant value, typically till $n_p \sim 10$.[18] This assumption, however, hardly affects product particle characteristics as primary particle diameter is determined largely by sintering, and agglomerate size is determined by coagulation that tends to "forget" or "mask" early particle characteristics. The error from a constant D_f is less than 10% even for $n_p = 3$.[21] When sintering is slow with respect to coagulation fractal like agglomerates are formed and D_f rapidly approaches a constant asymptotic value (for example, 1.8). Increasing sintering rates delay the formation of agglomerates slowing down the attainment of that asymptotic value of D_f.[20] Here a constant D_f will be used. This assumption slightly overpredicts the agglomerate diameter and even less the primary particle diameter.[22] It is balanced somehow by the assumption of monodispersity that tends to underpredict the coagulation rate,[23] and subsequently underpredicts also the product agglomerate particle diameter but hardly affects the primary particle diameter.[2]

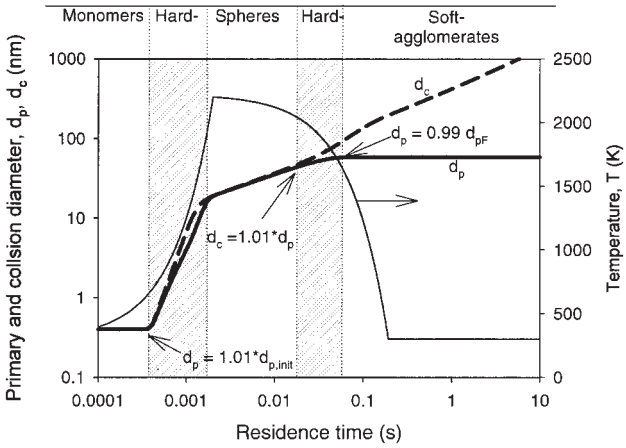

Figure 2. Evolution of the primary particle diameter (d_p, solid bold line), agglomerate collision diameter (d_c, broken bold line) and flame temperature (thin line) for TiO_2 formation by TTIP oxidation at T_{max} = 2,200 K, ϕ = 0.01, CR = 10,000 K/s, no surface growth.

The hard-agglomerate formation periods are highlighted by gray shading.

Results and Discussion

The influence of process parameters (maximum flame temperature T_{max}, cooling rate, CR (K/s), and precursor molar fraction, ϕ) on primary particle and agglomerate size and structure is investigated for titania formation by TTIP oxidation solving Eqs 1–4 along with the auxiliary functions in Eqs. 5–9. The flame temperature profile is defined by a linear increase from T = 300 K (at t = 0) to a maximum temperature T_{max} (= 2,000 – 2,400 K) reached within $t = t_{max} = 2$ ms, followed by a decrease to 300 K at a constant CR = $100 – 10^6$ K/s.[4] The employed molar fractions with respect to inlet precursor vapor, ϕ, lie between 0.001 (for laboratory reactors) up to 0.5 (for industrial ones). These conditions are typical for flame reactors (for example, Arabi-Katbi et al.[5]), and are chosen to ensure that the entire precursor has reacted completely at the end of the process providing a maximum process yield and avoiding release of valuable precursor, equivalent "chloride-slip" for TiO_2 formation by $TiCl_4$ oxidation.

Evolution of particle size and morphology

For an initial TTIP molar ratio $\phi = 0.01$, $t_{max} = 2$ ms, CR = 10^4 K/s and T_{max} = 2,200 K, and without accounting for surface reaction, Figure 2 shows the temperature profile (thin line) and the evolution of the corresponding d_p (bold solid line) and d_c (bold broken line). The evolution of particle diameters is consistent with what is known already showing the initial rapid growth of d_p until it levels off when sintering ceases while the d_c continues to grow by coagulation.

Figure 2 highlights with gray shading the periods of hard agglomerate formation that are defined when sintering takes place and d_c is larger than d_p. In detail, the following stages (periods) are observed: *Monomer period ($t < 0.5$ ms):* The primary particle diameter is essentially equal to the diameter of a single TiO_2 molecule (monomer) as only too few have been

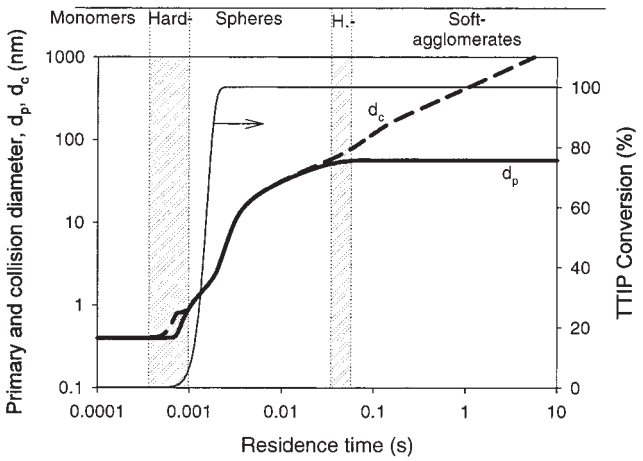

Figure 3. Evolution of the primary particle diameter (d_p, solid bold line), agglomerate collision diameter (d_c, broken bold line) and TTIP conversion (thin line) at the same conditions of Figure 2 accounting for surface growth.

Differences in the evolution of d_p and d_c are identified only at low residence times (<0.01 s) when compared with Figure 2. The hard agglomerate periods (gray-shading) shorten when accounting for surface growth that affects particle dynamics as long as the precursor is not fully converted.

formed; *Early Hard-Agglomerate formation period (t = 0.5–1 ms):* As temperature increases, chemical reaction produces molecules faster that collide forming clusters that do not fully coalesce as the temperature is not high enough for faster coalescence than collision. As a result agglomerates are formed that are hard as partial sintering takes place. The onset of that period is defined when d_c starts to exceed d_p and ends when the increasing temperature accelerates coalescence so that again $d_c = d_p$; *spherical or nonagglomerate particle formation period (t =1 – 50 ms):* Here the maximum process temperature is encountered resulting in much faster coalescence than collision rates leading to spherical particles; *late hard-agglomerate formation period (t =50 – 70 ms):* Now hard agglomerates are formed again as temperature drops enough for coalescence to become slower than particle collisions so again d_c becomes larger than d_p, as only partial sintering takes place. The onset of this period is defined when $d_c > 1.01\ d_p$; *soft-agglomerate formation period (t > 70 ms):* Here the temperature has dropped so much that sintering has effectively stopped (for example, $d_p > 0.99\ d_{pF}$ where d_{pF} is the final constant value of d_p). Coagulation, however, continues leaving the agglomerate surface area concentration and primary particle diameter essentially unchanged (within four digit accuracy[4]). The largest hard-agglomerate size d_H, is attained at t = 70 ms (end of late hard-agglomerate period) when $d_p = 0.99\ d_{pF}$. All agglomerates larger than this are held together with nonchemical (nonsinter) bonds, so when exposed to some stress (for example, shear), they will tend to break more easily than ones with chemical (sintered) bonds. It should be noted that soft-agglomerates are not discussed here as their constituent hard- or nonagglomerate particles are held together by weak physical bonds.

Effect of surface growth and initial precursor concentration

Figure 3 shows the evolution of d_p and d_c for the conditions of Figure 2, but accounting now for surface growth. Comparing these figures, the large influence of surface growth on the evolution of d_p and d_c is seen within the early particle formation stages (up to 60 ms). The d_p increases a bit slower, and the onset of fully coalescent agglomeration (starting at 1 ms) occurs earlier and again turns into hard agglomeration later (at 60 ms) than in the case without surface growth. As a result, the hard agglomeration periods (grey zones) are shorter when accounting for surface growth. The latter suppresses gas phase reaction (Eq. 11) resulting in smaller (initial) early hard-agglomerates which later on produce smaller spherical particles when they coalesce. Interestingly, both the end of the second (late) hard agglomeration period at 70 ms and the hard agglomerate dia. d_H are not influenced by surface growth. Consequently, the degree of agglomeration h, is not affected by surface growth. This is not surprising as long as chemical reaction has been completed before the end of sintering as precursor oxidation has been completed at 2 ms while sintering at 70 ms.[4]

Figure 4 shows the evolution of d_p and d_c for the conditions of Figure 3 (accounting for surface growth), but at higher inlet precursor concentration, $\phi = 0.1$. This leads to a higher particle concentration in the flame that increases agglomeration consistent with Eq. 2. As a result, d_p increases faster reaching sizes quickly for which sintering is rather slow at this temperature.[13] Subsequently, when comparing with Figure 3 an early onset (at 6 ms) of the late hard agglomeration period is observed with increasing ϕ. Although this hard agglomeration period ends earlier than in Figure 3, larger hard-agglomerates are formed consistent with the faster agglomeration rates at $\phi = 0.1$ than at 0.01. Furthermore, this leads to a significant increase of the collision diameter at the end of the hard-

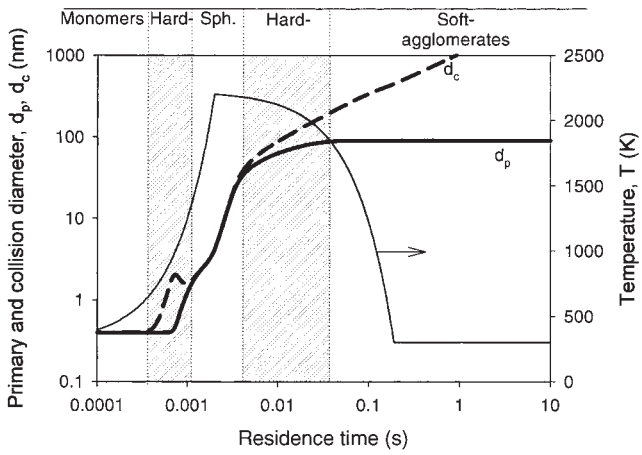

Figure 4. Evolution of the primary particle diameter (d_p, solid bold line) and the agglomerate collision diameter (d_c, broken bold line) together with flame temperature (thin line) for the conditions of Figure 3, but $\phi = 0.1$.

The precursor concentration affects particle formation, and most notably the agglomeration state of the product particles.

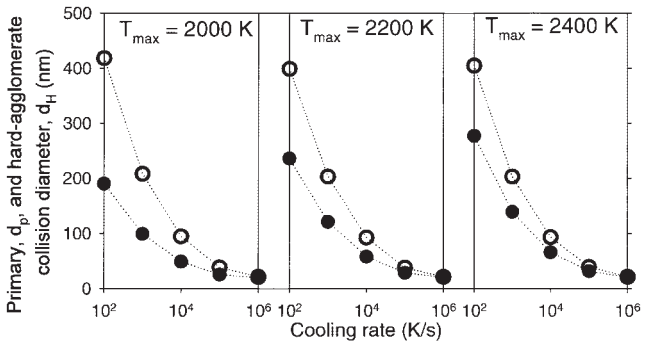

Figure 5. Primary particle diameter (filled symbols) and hard agglomerate collision diameter (open symbols) as a function of the cooling rate for three maximum process temperatures (2,000 K, 2,200 K and 2,400 K) at $\phi = 0.01$ and surface growth.

agglomeration period, d_H, increasing the degree of hard-agglomeration h, of the product particles.

Hard-Agglomeration Maps

Figure 5 shows the primary particle diameter and the hard-agglomerate collision diameter evaluated for three maximum flame temperatures (T_{max} = 2,000, 2,200 and 2400 K), as a function of cooling rate (CR = 100 – 10^6 K/s) at a constant precursor concentration (ϕ = 0.01). Whereas an increase of maximum flame temperature increases the hard primary particle diameter and does not significantly change the hard agglomerate collision diameter, an increase in cooling rate significantly decreases both d_p and d_H but mostly the latter. Therefore, the degree of hard agglomeration, decreases with increasing maximum flame temperature and increasing cooling rate. One can see that rather small, but fully spherical hard particles can always be produced at very high cooling rates (10^6 K/s) and ϕ = 0.01 as has been observed also for high-temperature synthesis of SiO_2.[4]

Figure 6 summarizes the degree of hard-agglomeration h as a function of cooling rate CR, and initial precursor volume fraction, ϕ, for four T_{max} covering the operational range of flame synthesis of TiO_2 by TTIP oxidation. The observed results are given in form of agglomeration maps showing contour plots of the degree of hard-agglomeration superimposed by isopleths of the corresponding primary particle diameter (yellow lines). Generally, particles with a low degree of hard-agglomeration can be produced when using high cooling rates and low precursor concentrations. At higher temperatures, the region of low degree of agglomeration is extended to higher precursor concentrations. Furthermore, agglomerates with small primary particles tend to be less agglomerated than those with large primary particles. This can be explained by the fact that the sintering rate depends strongly on the primary particle size, and is faster for small primary particles.

Thus, nonagglomerated particles can be produced at a relatively low feed fraction and a high cooling rate. These maps could help find appropriate process conditions for one-step production of particles with desired properties. For a practical system, the easiest parameter to control is the precursor concentration. Because particle manufacture at low precursor concentrations is often economically disadvantageous, the cooling rate and flame maximum temperature are more attractive operation parameters. These can be controlled, for example, by reactant mixing[24], precursor composition, cold gas injection[25], flow through an expansion nozzle[26] or even external electric fields.[27]

Comparison with experimental data

Figure 6 shows also experimental data on TiO_2 formation by TTIP oxidation in premixed flames that have been obtained consistently: Data analysis includes thermophoretic sampling and transmission electroscope imaging for particle sizing and IR-spectroscopy for flame temperature measurements. Using the T_{max} reported and extracting average cooling rates for each data set, the corresponding degrees of hard agglomeration are estimated and included into the agglomeration maps (Table 1). For calculation of the average cooling rates the reported temperature — distance profiles were transformed into time-dependent profiles. The necessary gas velocity was evaluated at the nozzle from given data and was corrected for temperature by ideal gas law. The average cooling rate was then evaluated by linearization giving a good representation of the measured temperatures. Experimentally, it is difficult to distinguish between hard and soft agglomerates because, when dealing with nanoparticles, even van der Waals bonding present in soft agglomerates may not be broken by shear. Most *ex situ* particle size measurements only give information of the primary particle diameter (for example, nitrogen adsorption, X-ray diffraction). However, insight into the hard-agglomerate structure is available from transmission-electron spectroscopy (with limitations), optical methods (SAXS) and measurements in suspensions (dynamic light scattering, settling velocities[28]) as much higher shear rates are achievable in thin tubes and by high-energy sonication.

For all experimental data investigated here nearly spherical titania particles are reported (h $\sim$ 1) from TEM imaging. Figure 6 shows good agreement between the maps and the data

Table 1. Conditions for Synthesis of Hard- and Non-Agglomerated TiO_2 Particles in Premixed Flames

T_{max} (K)	CR (K/s)	ϕ	d_p	TiO_2 Data and Temperature Profiles
2000	60′000	0.001	25	Arabi-Katbi et al.,[5]4 g/h: Figs. 4 & 5
2200	100′000	0.003	35	11 g/h: Figs. 4 & 6
2300	70′000	0.004	45	15 g/h: Figs. 4 & 8
2400	100′000	0.005	40	Tsantilis et al.,[2] Figs. 4 & 7
2400	20′000	0.01	70	Kammler et al.,[27] 11 g/h: w/o elect. field, Fig. 5
2400	30′000	0.01	50	w. elect. field, Fig. 7
1200	20′000	0.001	20	Diffusion flame: Pratsinis et al.[24]
2000	20′000	0.001	100	Johannessen et al.,[12] Fig. 3 & Table 1

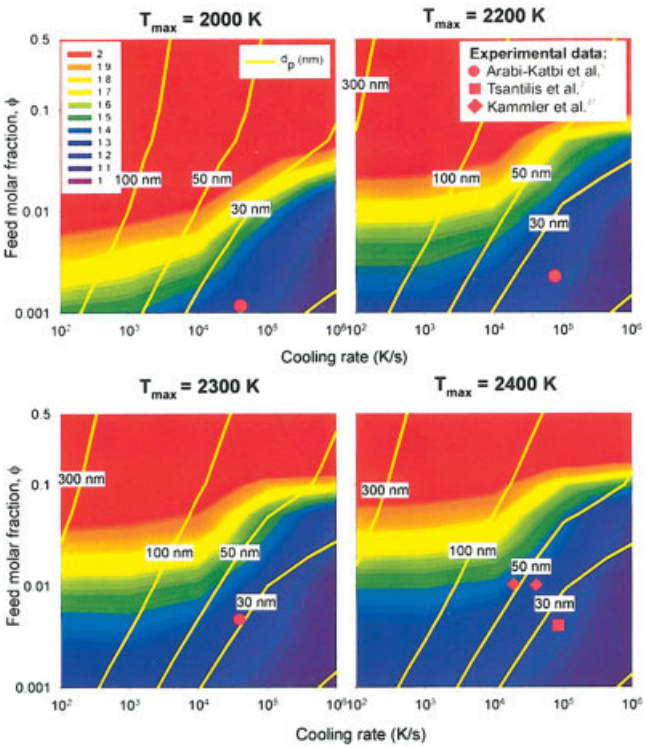

Figure 6. Titania agglomeration maps ($h = d_H/d_p$) in terms of initial TTIP molar feed fraction, ϕ, and average cooling rate (CR) for 4 maximum temperatures including surface growth.

The thin yellow lines indicate isopleths of primary particle size. Red symbols indicate the d_p of nonagglomerated TiO_2 particles from the literature. Decreasing ϕ, and to lesser extent increasing T_{max} and CR, reduces the degree of TiO_2 agglomeration.

regarding the primary particle diameter d_p and degree of agglomeration. It should be noted that the good agreement between model and experiments for d_p has been reported previously.[2] Both the influence of the precursor concentration and the cooling rate are correctly predicted: Arabi-Katbi et al.[5] report an increasing primary particle size with increasing initial precursor concentration; in addition, Kammler et al.[27] investigating the influence of electrical fields on titania formation present an increasing cooling rate when applying the electrical field resulting in smaller and essentially nonagglomerated, spherical particles consistent with Figure 6 (T_{max} = 2,400 K). Although all experimental data are confined at rather low precursor concentrations, trends are consistent with the calculations reported here.

A set of experimental conditions leading to highly agglomerated titania particles could be found for $TiCl_4$ oxidation in different diffusion flame configurations.[24] This set of experimental conditions had been analyzed by Hyeon-Lee et al.[29] giving information on particle morphology by SAXS (small-angle X-ray scattering) measurements and by Johannessen et al.[12] giving flame temperature profiles from fluid dynamic calculations. Therefore, to validate this model with agglomerated TiO_2 also, an agglomeration map in terms of ϕ and T_{max} (instead of CR) was prepared for a $TiCl_4$ precursor assuming instantaneous reaction (Figure 7). Using the temperature profile from Johannessen et al.[12] (T_{max} = 1,200 and 2,000 K at the axis of flames B and D, respectively, CR = 20,000 K/s and a time to T_{max} of 0.05 s) together with the feed molar fraction of[24] ~0.001. Figure 7 predicts that flame D produces nonagglomerated particles with h = 1 (triangle) while flame B produces hard agglomerates with h~25 (circle) These calculated degrees of agglomeration are consistent with SAXS measurements[29] showing that particles produced by high-temperature flame D are spherical (n_p = 1), while particles produced by low temperature flame B are dense hard- agglomerates (n_p = 29). It should be noted the calculated primary particle diameters are smaller than those measured.[24] Johannessen et al.[12] obtained a better agreement with theory accounting for the variable residence time of the diffusion flame and by employing a two stage TiO_2 sintering model.

Comparison with hard-agglomeration maps for silica

When comparing the agglomeration maps presented here (Figure 6) with those for silica made similarly by $SiCl_4$ oxidation (Tsantilis and Pratsinis[4]: Figure 8) large and even qualitative differences are observed. One can draw the conclusion that titania particles generally attain a higher degree of agglomeration than those of silica for a wider range of cooling rates, maximum process temperatures and initial precursor volume fractions. This is clearly shown, for instance for T_{max} = 2,200 K, where the red-orange region is more widespread for titania than for silica. Titania formation is less sensitive to varying temperature conditions (T_{max} and CR). Highly agglomerated titania are made always at high-feed molar fractions. Similarly, titania nanoparticles are often reported as nonagglomerated nearly independent of experimental process conditions as long

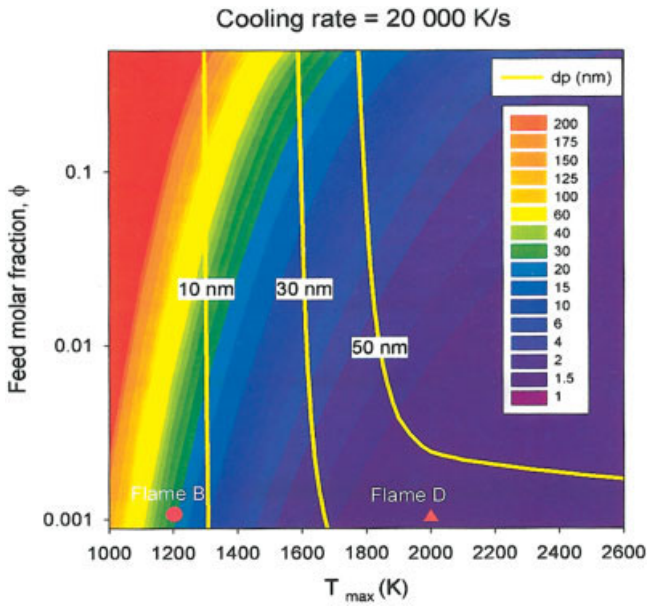

Figure 7. Titania hard-agglomeration maps ($h = d_H/d_p$) in terms of initial $TiCl_4$ molar fraction, ϕ, and maximum flame temperature for a cooling rate of 20'000 K/s including surface growth.

The thin yellow lines indicate isopleths of primary particle size. Comparison with experimental data[12,24,29] is shown as a red dot (for flame setup B) and triangle (for flame setup D).

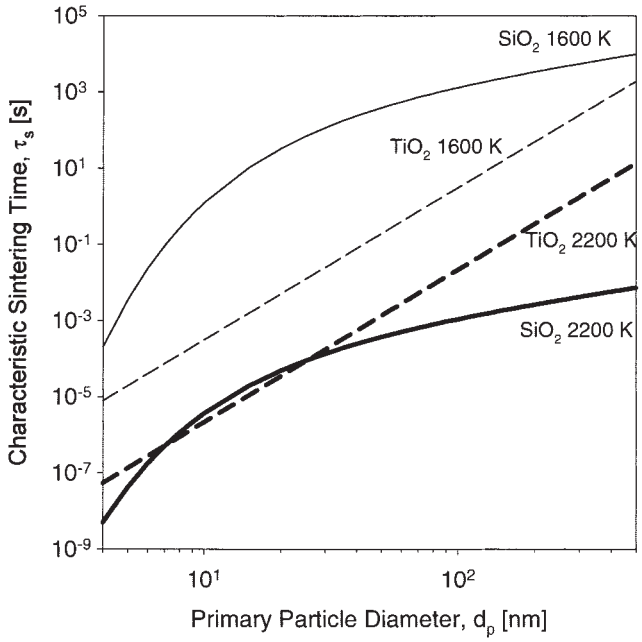

Figure 8. Characteristic sintering times for TiO_2 (broken lines) and SiO_2 (solid lines) according to equation (5) and Tsantilis et al.[32], respectively, for 1,600 K (thin lines) and 2,200 K (bold lines).

At relatively low-temperatures, SiO_2 sinters slower than TiO_2, a trend that is reversed at high-temperatures. Furthermore, SiO_2 is more sensitive to temperature than TiO_2.

as low concentrations are employed at these T_{max} (for example, Arabi-Katbi et al.[5]). In contrast the degree of silica agglomeration can be controlled by varying these process conditions (for example, Mueller et al.[30]: Figure 2).

The reason for this difference stems from the differing sintering rates even though both silica and titania dynamics are described by the same differential equations. The sintering rate is the main material parameter controlling the formation of agglomerates. Figure 8 shows the characteristic sintering time for both silica (solid lines) and titania nanoparticles (broken lines) at 1,600 K (thin lines), and 2,200 K (bold lines). Here, the large difference in morphology between silica and titania particles becomes apparent as the sintering times depend differently on temperature and primary particle diameter: Whereas with titania there is only little influence of temperature on the sintering time, this is substantial for silica. For moderate to low cooling rates ($CR < 2{,}000$ K/s) and, thus, for temperatures close to T_{max}, the characteristic sintering time of silica (Figure 8, bold solid line) is smaller than the corresponding one for titania (Figure 8, bold broken line) especially for primary particle sizes bigger than 100 nm enabling the formation of such particles with a lower degree of agglomeration. However, this trend is reversed at high cooling rates ($CR > 10^5$ K/s), as the temperature drops faster to lower levels slowing down coalescence of silica more significantly than in the case of titania (Figure 8, thin lines). As a result one would expect the development of sintering bonds and, subsequently, hard agglomerates to larger extent in SiO_2 than in TiO_2 experiencing the same high-temperature residence time history, (for example, Xiong et al. 1993: Figure 5).[31]

Concluding Remarks

Hard-agglomerates are particles held together strongly, for example, by chemical or sinter bonds (necks), while soft-ones are bonded rather weakly, for example, by physical or van der Waals forces. The evolution of hard- and soft-agglomerate TiO_2 particles made by gas phase and surface oxidation of titanium isopropoxide was investigated theoretically and compared to literature data. Hard-agglomerates with low degree of agglomeration or even nonagglomerates could be produced at low-feed molar fractions, high-maximum process temperature and, to a lesser extent, at high-cooling rates. Accounting for surface reactions affected the early stage of particle growth by starting earlier the formation of hard agglomerates, but had practically no effect on the degree of agglomeration of the product particles as reaction had been completed well before the end of sintering at the conditions studied. The model predictions in the form of hard-agglomeration maps were consistent with experimental data of nonagglomerate TiO_2 particles (25 - 70 nm) made by TTIP and $TiCl_4$ oxidation in premixed flames and even with hard-agglomerated TiO_2 made by $TiCl_4$ oxidation in diffusion flames. These agglomeration maps show that the degree or extent of agglomeration can be addressed with a few process variables. It should be understood, however, that newly-formed particles traverse a temperature profile (simplified here by T_{max}, and a linear cooling rate) which has a profound effect on the agglomerate structure of the product.

Acknowledgments

This article was presented at the AIChE Annual Meeting, Austin, TX, Nov. 7-12, 2004. Partial support by the Swiss National Foundation is acknowledged gratefully.

Literature Cited

1. Shannon RD, Pask JA. Kinetics of anatase-rutile transformation. *J of the American Ceramic Soc.* 1965;48:391-394.
2. Tsantilis S, Kammler HK, Pratsinis SE. Population balance modeling of flame synthesis of titania nanoparticles. *Chem Eng Sci.* 2002;57:2139-2156.
3. Vemury S, Pratsinis SE. Self-preserving size distributions of agglomerates. *J of Aerosol Sci.* 1995;26:701-701.
4. Tsantilis S, Pratsinis SE. Soft- and hard-agglomerate aerosols made at high temperatures. *Langmuir.* 2004;20:5933-5939.
5. Arabi-Katbi OI, Pratsinis SE, Morrison PW, Megaridis CM. Monitoring the flame synthesis of TiO2 particles by in-situ FTIR spectroscopy and thermophoretic sampling. *Combustion and Flame.* 2001;124:560-572.
6. Windeler RS, Lehtinen KEJ, Friedlander SK. Production of nanometer-sized metal oxide particles by gas phase reaction in a free jet.2. Particle size and neck formation - Comparison with theory. *Aerosol Sci and Technol.* 1997;27:191-205.
7. Kruis FE, Kusters KA, Pratsinis SE, Scarlett B. A Simple-model for the evolution of the characteristics of aggregate particles undergoing coagulation and sintering. *Aerosol Sci and Technol.* 1993;19:514-526.
8. Landgrebe JD, Pratsinis SE. A discrete-sectional model for particulate production by gas-phase chemical-reaction and aerosol coagulation in the free-molecular regime. *J of Colloid and Interface Sci.* 1990;139:63-86.
9. Xiong Y, Pratsinis SE. Formation of agglomerate particles by coagulation and sintering.1. A 2-Dimensional solution of the population balance equation. *J of Aerosol Sci.* 1993;24:283-300.
10. Jeong JI, Choi M. A simple bimodal model for the evolution of non-spherical particles undergoing nucleation, coagulation and coalescence. *J of Aerosol Sci.* 2003;34:965-976.
11. Schild A, Gutsch A, Muehlenweg H, Kerner D, Pratsinis SE. Simu-

lation of nanoparticle production in premixed aerosol flow reactors by interfacing fluid mechanics and particle dynamics. *J of Nanoparticle Res.* 1999;1:303-315.
12. Johannessen T, Pratsinis SE, Livbjerg H. Computational analysis of coagulation and coalescence in the flame synthesis of titania particles. *Powder Technol.* 2001;118:242-250.
13. Kobata A, Kusakabe K, Morooka S. Growth and transformation of TiO_2 crystallites in aerosol reactor. *AIChE J.* 1991;37:347-359.
14. Seinfeld JH. *Atmospheric chemistry and physics of air pollution*. New York: Wiley; 1986.
15. Okuyama K, Ushio R, Kousaka Y, Flagan RC, Seinfeld JH. Particle generation in a chemical vapor-deposition process with seed particles. *AIChE J.* 1990;36:409-419.
16. Battiston GA, Gebrasi R, Guerrra M, Porchia M. Gas-phase FT-IR analysis and growth kinetics of TiO2 in a hot wall LP-MOCVD reactor. Chemical Vapor Deposition*, Proceedings of the Fourtheenth International CVD Converence and EUROCVD-11.* In M. D. Allendorf, & C. Bernard, Eds. Vol 97-25. Pennington, NJ: Elecrochemical Society; 1997.
17. Schaefer DW, Hurd AJ. Growth and structure of combustion aerosols - Fumed silica. *Aerosol Sci and Technoly.* 1990;12:876-890.
18. Mitchell P, Frenklach M. Particle aggregation with simultaneous surface growth. *Physical Review E.* 2003;67:Art. No. 061407.
19. Beaucage G, Kammler HK, Mueller R, Strobel R, Agashe N, Pratsinis SE, Narayanan T. Probing the dynamics of nanoparticle growth in a flame using synchrotron radiation. *Nature Materials.* 2004;3:370-374.
20. Akhtar MK, Lipscomb GG, Pratsinis SE. Monte-carlo simulation of particle coagulation and sintering. *Aerosol Sci and Technol.* 1994;21: 83-93.
21. Lattuada M, Wu H, Morbidelli M. A simple model for the structure of fractal aggregates. *J of Colloid and Interface Sci.* 2003;268:106-120.
22. Artelt C, Schmid HJ, Peukert W. On the relevance of accounting for the evolution of the fractal dimension in aerosol process simulations. *J of Aerosol Sci.* 2003;34:511-534.
23. Hinds W. *Aerosol Technology*. New York: Wiley-Interscience; 1999.
24. Pratsinis SE, Zhu WH, Vemury S. The role of gas mixing in flame synthesis of titania powders. *Powder Technol.* 1996;86:87-93.
25. Hansen JP, Jensen JR, Livbjerg H, Johannessen T. Synthesis of ZnO particles in a quench-cooled flame reactor. *AIChE J.* 2001;47:2413-2418.
26. Wegner K, Stark WJ, Pratsinis SE. Flame-nozzle synthesis of nanoparticles with closely controlled size, morphology and crystallinity. *Materials Letts.* 2002;55:318-321.
27. Kammler HK, Jossen R, Morrison PW, Pratsinis SE, Beaucage G. The effect of external electric fields during flame synthesis of titania. *Powder Technol.* 2003;135:310-320.
28. Grass RN, Stark WJ. Flame synthesis of calcium-,strontium-, barium fluoride nanoparticles and sodium chloride. *Chem Communications.* 2005:1767-1769.
29. Hyeon-Lee J, Beaucage G, Pratsinis SE, Vemury S. Fractal analysis of flame-synthesized nanostructured silica and titania powders using small-angle X-ray scattering. *Langmuir.* 1998;14:5751-5756.
30. Mueller R, Kammler HK, Pratsinis SE, Vital A, Beaucage G, Burtscher P. Non-agglomerated dry silica nanoparticles. *Powder Technol.* 2004;140:40-48.
31. Xiong Y, Akhtar MK, Pratsinis SE. Formation of agglomerate particles by coagulation and sintering.2. The evolution of the morphology of aerosol-made titania, silica and silica-doped titania powders. *J of Aerosol Sci.* 1993;24:301-313.
32. Tsantilis S, Briesen H, Pratsinis SE. Sintering time for silica particle growth. *Aerosol Sci and Technol.* 2001;34:237-246.

Manuscript received Mar. 24, 2005, and revision received Sept. 16, 2005.